NASA CONTRACTOR REPORT

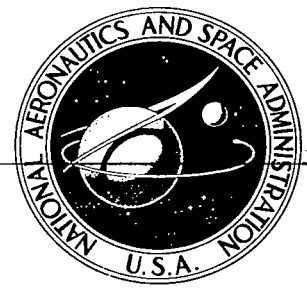

ON MINIMIZING THE WAKE OF DROPLETS

by Franklin K. Moore

Prepared by
CORNELL UNIVERSITY
Ithaca, N. Y.
for Lewis Research Center

NATIONAL AERONAUTICS AND SPACE ADMINISTRATION • WASHINGTON, D. C. • MAY 1969

NASA CR-1368

ON MINIMIZING THE WAKE OF DROPLETS

By Franklin K. Moore

Prepared under Grant No. NGR-33-010-042 by
CORNELL UNIVERSITY
Ithaca, N.Y.

for Lewis Research Center

NATIONAL AERONAUTICS AND SPACE ADMINISTRATION

For sale by the Clearinghouse for Federal Scientific and Technical Information
Springfield, Virginia 22151 – CFSTI price $3.00

FOREWORD

The research described herein, which was conducted at Cornell University, Department of Thermal Engineering, was performed under NASA Grant NGR-33-010-042 with Dr. John C. Evvard, NASA Lewis Research Center, as Technical Monitor.

SUMMARY

The inviscid flow inside and outside a moving droplet is analyzed, allowing the shape to be nonspherical subject to surface tension. Specifically, the Weber number-drag relationship is sought which seems to assure the least tendency to form a separated wake. Two conditions of continuous velocity derivatives are imposed at the rear stagnation point for this purpose.

The results give reasonable changes of shape (flattening) and reasonable but somewhat too low values of Weber number for minimum wake.

Even rather small departures from spherical shape dramatically suppress internal circulation.

INTRODUCTION

There is a continuing interest in the fluid mechanics of droplets of one fluid moving through a different fluid. Perhaps the chief technological reason for this interest has to do with combustion processes involving the dispersal of one fluid in another. The present study has a somewhat general motivation in terms of fluid confinement. There are many reasons why one might wish a flow to proceed in such a way as to preserve the separation between two different fluids. There are two real fluid considerations, at least, which must be considered in such a study. First, there must be a shape-stabilizing mechanism such as surface tension. Electromagnetic pinch and rotational inertia may also be effective in this respect. In the present study, we accept surface tension as a prototype of such restraining influences.

The second, more mysterious effect is that of viscosity. We must assume that no self confined flow can last forever; it must ultimately be destroyed by viscosity, heat conduction, and diffusion, or a combination of these. This report concerns the most obvious effect of viscosity, that is, the tendency of the flow on the rearward part of an object to separate which, in addition to producing drag of the object as a whole, presumably would contribute to the decay of the internal motions of the droplet.

Recent papers by Winnikow and Chao (Ref. 1) and Harper and Moore (Ref. 2) have dealt with various aspects of droplets at high Reynolds number. In both these papers, the theory begins with the inviscid flow comprising a Hill's vortex inside the droplet, and a potential flow outside. The droplet is considered spherical, and the theories proceed to consider the viscous boundary layer connecting these inner and outer flows.

The most troublesome aspect of these theories is the treatment of the vicinity of the rear stagnation point where flow separation and eddy formation, both inside and outside the droplet, may or may not occur.

The variety of possibilities is indicated by the experimental results of Winnikow and Chao. Even in the same Reynolds number range the wake may be a very narrow thread or a much wider region of disturbance, depending, in effect, on the size of the droplet. It proves difficult to sort out the factors influencing wake size. For example, one might expect separation to depend on Reynolds number (boundary layer thickness) and Weber number (degree of flattening of the droplet). However, since in the experiments, drag is always in balance with gravity, a change of droplet mass changes both Reynolds and Weber numbers, and the effects are difficult to separate.

In the present note we consider inviscid flow (infinite Reynolds number), but allow shape to change because of surface tension, and ask if there is any Weber number for which the inviscid flow would be expected to have features associated with a small or vanishing wake.

EQUATIONS OF THE PROBLEM

We assume an axisymmetric flow in which vorticity is fully diffused; that is, in keeping with Batchelor's theorem (Ref. 3), the vorticity is proportional to distance from the axis of symmetry within the droplet. The differential equation for the stream function is

$$\Psi_{rr} - \frac{\cot\theta}{r^2}\,\Psi_\theta + \frac{1}{r^2}\,\Psi_{\theta\theta} = kr^2\sin^2\theta \tag{1}$$

where

$$u = \frac{\partial\Psi/\partial\theta}{r^2\sin\theta} \quad ; \quad v = \frac{\partial\Psi/\partial r}{r^2\sin\theta} \tag{2}$$

A sketch of coordinates appears in Fig. 1. Outside the droplet, where the flow is irrotational, Eq. 1 applies with the right-hand side omitted ($k \equiv 0$).

The boundary conditions used with these equations are the following: There is a uniform stream of velocity U far from the droplet

$$\lim_{r\to\infty} \frac{\partial\Psi_0/\partial r}{r(1-\mu^2)} = U \quad ; \quad \mu \equiv \cos\theta \tag{3}$$

where the subscript zero denotes flow quantities outside the droplet. Subscript i will denote flow quantities inside the droplet. Thus, the specification that the droplet surface is a stream surface for both inner and outer flows may be written

$$\Psi_0(R(\theta),\theta) = \Psi_i(R(\theta),\theta) = 0 \tag{4}$$

where $R(\theta)$ defines the surface of the droplet. Finally, across the droplet surface, pressure must balance surface tension. For a given shape $R(\theta)$, pressure difference due to surface tension would be

$$\left(\frac{p_i-p_o}{\rho}\right)_R = \frac{R(2R^2+3R'^2-RR'')\sin\theta - R'(R^2+R'^2)\cos\theta}{R(R^2+R'^2)^{3/2}\sin\theta} \tag{5}$$

If R is constant this formula reduces to the correct result, namely, 2/R. The pressure difference obtained from the Bernoulli equation, including buoyancy force, would be

$$\left(\frac{p_i-p_o}{\sigma}\right)_R = \frac{K}{R_1} - \mu R g\frac{\rho_i-\rho_o}{\sigma} - \frac{\rho_i}{2\sigma R^2(1-\mu^2)}\left[\left(\Psi_{i_r}^{\ 2} + \frac{1}{R^2}\Psi_{i_\theta}^{\ 2}\right) - \frac{\rho_o}{\rho_i}\left(\Psi_{o_r}^{\ 2} + \frac{1}{R^2}\Psi_{o_\theta}^{\ 2}\right)\right] \tag{6}$$

Although we assume the flow to be incompressible inside and outside the droplet, the density is considered constant in both regions.

We may note at this point that the problem is not yet fully determined for a given droplet volume and velocity. Specifically, one may say that the vorticity inside the droplet is not yet fixed because of the possibility of various droplet shapes. If the droplet were spherical, the Bernoulli constant K would be determined immediately from Eqs. 5 and 6. In general, however, there must be a relationship between k, K and droplet shape that would admit various combinations of those parameters.

Presumably the problem is made determinate through the action of viscosity. Without attempting to analyze the viscous effects associated with the boundary of the above droplet, let us require that the velocity jump across the droplet surface have vanishing gradient at the rear stagnation point:

$$\lim_{\theta\to 0}\left(\frac{\partial\Psi_o/\partial r}{1-\mu^2}\right)_R = \lim_{\theta\to 0}\left(\frac{\partial\Psi_i/\partial r}{1-\mu^2}\right)_R \tag{7}$$

This boundary condition presumably makes the problem unique. In any droplet motion, the terminal flow situation must be partly the result of some effect of viscosity involving recirculation of vorticity within the droplet. Eq. 7, in effect, minimizes the tendency to flow separation at the rearward part of the droplet. That is, a boundary layer in that region would not be needed to compensate for a velocity discontinuity, and we know from the boundary-layer analysis of Chao (Ref. 4) that no flow separation occurs when there is no velocity jump in the purely spherical case.

At this point we could proceed to solve the system of equations and boundary conditions. However, since we are interested in finding conditions for the least effect of viscosity, we add an additional boundary condition to the effect that there is no surface gradient of shear-stress discontinuity at the rear stagnation point. In effect, the generation of vorticity is assumed to vanish at $\theta = 0$. The following condition, then, represents what would seem to be the greatest possible suppression of viscous effects associated with wake formation:

$$\lim_{\theta\to 0}\left[\frac{\mu_o}{\sin^2\theta}\left(\frac{\partial}{\partial r}-\frac{1}{R_c}\right)\left(\frac{1}{r}\frac{\partial\psi_o}{\partial r}\right)\right]_R = \lim_{\theta\to 0}\left[\frac{\mu_i}{\sin^2\theta}\left(\frac{\partial}{\partial r}-\frac{1}{R_c}\right)\left(\frac{1}{r}\frac{\partial\psi_i}{\partial r}\right)\right]_R \tag{8}$$

where R_c is the radius of curvature of the surface at the rear stagnation point. Presumably this additional boundary condition will lead to a relationship between Weber and Bond numbers, for example, that would identify conditions for a minimum wake.

SOLUTION OF THE EQUATIONS

Solutions to Eq. 1 may be written in terms of spherical harmonics as follows:

$$\psi_i = (1-\mu^2)\left[-\frac{k}{2}\mu^2 r^4 + \sum_1^\infty A_n r^{n+1} P_n'(\mu)\right] \tag{9}$$

$$\psi_o = (1-\mu^2)\left[\tfrac{1}{2}Ur^2 = \sum_1^\infty C_n r^{-n} P_n'(\mu)\right] \tag{10}$$

where the P_n are the Legendre polynomials. Inside the droplet terms singular at the origin have been dropped, while outside, terms singular at infinity have been dropped. For convenience, the following definitions are made:

$$\left.\begin{aligned} \kappa &\equiv kR_1^2/U \\ a_n &\equiv A_n R_1^{n-1}/U \\ c_n &\equiv C_n R_1^{-n-2}/U \\ W &\equiv \rho_o U^2 R_1/2\sigma \\ B &\equiv (\rho_i-\rho_o)gR_1^2/4\sigma \end{aligned}\right\} \quad (11)$$

Parenthetically, we may note that Hill's spherical vortex is a particular case of Eq. 9, where

$$\kappa = -7\tfrac{1}{2}\ ; \qquad a_1 = 3/4\ ; \quad a_3 = -1/2 \qquad (12)$$

and the other coefficients vanish. We may obtain a simple approximate solution by truncating the series of Eqs. 9 and 10, keeping only the first three terms of the sums. Correspondingly, we apply boundary conditions at only three points -- the rear stagnation point, the shoulder ($\theta = \pi/2$), and the forward stagnation point. We assume an interpolation formula for radius of the droplet, quadratic in μ, designed to pass through the three points defining the shape of the droplet. R_2 and R_3 may be regarded as unknown, while R_1, in effect, is used to define the size of the droplet.

$$R = R_2 + 1/2(R_1-R_3)\mu + 1/2(R_1-2R_2+R_3)\mu^2 \qquad (13)$$

Before proceeding let us count unknowns and equations. Three A's, three C's, and two radii account for eight unknowns. κ (the level of vorticity), K (the Bernoulli constant or pressurization of the droplet) and Weber number (W) add three additional unknowns for a total of 11. Turning to the boundary conditions, requiring points 1, 2 and 3 to be on stream surfaces of both inner and outer flows yields six conditions. The balance of pressure and surface tension at those three points, together with the two special conditions at the rear stagnation point, give a total of 11 equations, which should suffice to determine the 11 unknowns. We may write down the results of applying the first eight boundary conditions as follows. The "Bond number" B is a parameter of the problem.

$$R_2 = \frac{R_1+R_3}{4} + \frac{R_3}{R_1+R_3} - \frac{R_3^2}{R_1-R_3}\,B \qquad (14a)$$

$$K = 4B+1+2\frac{R_2}{R_1} - \frac{R_3}{R_1} \tag{14b}$$

$$a_2 = \frac{R_1-R_3}{3R_3}\, a_1 \tag{14c}$$

$$a_3 = \frac{2R_1^{\,2}}{3R_2^{\,2}}\, a_1 \tag{14d}$$

$$c_1 = -\frac{1}{2R_1^{\,3}}\,\frac{R_1^{\,5}-R_3^{\,5}}{R_1^{\,2}-R_3^{\,2}} - \frac{3R_1}{R_1-R_3}\, c_1 \tag{14e}$$

$$c_2 = \frac{(R_1^{\,5}+4R_2^{\,5})(R_1^{\,2}-R_3^{\,2}) - (R_1^{\,2}+4R_2^{\,2})(R_1^{\,5}-R_3^{\,5})}{3\quad (R_1+R_3)(R_1R_3+4R_2^{\,2})} \tag{14f}$$

$$c_3 = -\frac{1}{12}(1+2c_1+6c_2) \tag{14g}$$

$$\kappa = 2a_1\left(1+4\frac{R_1^{\,2}}{R_2^{\,2}}\right)+ 6a_2 \tag{14h}$$

We then apply Eq. 7 and find

$$a_1 = -\frac{R_3}{R_1+R_3}\left(\frac{5}{2} - 2c_1 + 3c_2\right) \tag{15}$$

In this set of equations, one may say that only one quantity, say R_3, remains unknown. Only two conditions remain: The pressure-surface tension balance at the shoulder of the droplet yields

$$W = \{\frac{4}{R_1+R_3} + 4B(R_1+\frac{R_3^2}{R_1-R_3}) - R_1\frac{2R_2^2+3/4(R_1-R_3)^2-R_2(R_1-2R_2+R_3)}{[R_2^2+1/4(R_1-R_3)^2]^{3/2}}\} \times$$

$$\{\frac{\rho_i}{\rho_o}[9a_2{}^2\frac{R_2^2}{R_1^2} + (2a_1-6a_3\frac{R_2^2}{R_1^2})^2]-[\frac{9c_2^2}{6}R_1^6 + (1-c_1\frac{R_1^3}{R_2^3} + \frac{gc_3R_1^5}{2R_2^5})^2]\}^{-1} \quad (16)$$

and finally the condition of Eq. 8 closes the system:

$$\frac{\mu_i}{\mu_o}[2a_1(4-\frac{R_1}{R_c}) + 3a_2(7-3\frac{R_1}{R_c})] = \frac{5}{2}(3+\frac{R_1}{R_c}) + 2c_1(6+\frac{R_1}{R_c}) + 3c_2(7+\frac{R_1}{R_c}) \quad (17)$$

Based on Eq. 13, the radius R_c may be written as

$$\frac{R_1}{R_c} = \frac{5}{2} - 2\frac{R_2}{R_1} + 1/2\frac{R_3}{R_1} \quad (18)$$

RESULTS AND DISCUSSION

The solution of the foregoing system of algebraic equations was obtained on a high-speed computing machine for the liquid combinations featured in Ref. 1. Results have been calculated in terms of an equivalent drop radius, that is, the radius of the sphere that would have the same volume as the drop.

$$\frac{4}{3}\pi R_e^3 \equiv \text{volume of drop} \quad (19)$$

Bond and Weber numbers are then expressed in terms of this equivalent radius:

$$B' \equiv (\frac{R_e}{R_1})^2 \; ; \quad W' \equiv W\frac{R_e}{R_1} \quad (20)$$

and we calculate a drag coefficient based on the equivalent frontal area of the droplet.

$$C_D \equiv \frac{D}{1/2\rho U^2 \pi R_e^2} \tag{21}$$

and assume that the drag is that necessary to balance negative buoyancy.

$$D = (\rho_i - \rho_o) g \frac{4}{3} \pi R_e^3 \tag{22}$$

Thus, the drag coefficient is a ratio of Bond to Weber numbers, and perhaps, more properly, should be called a Froude number.

$$C_D = \frac{16}{3} \frac{B'}{W'} \tag{23}$$

It should be obvious that the drag coefficient calculated in this way is not necessarily that which will actually be produced by the action of viscosity.

The results of the calculations are compiled in the Table, for four different combinations of substances. In each case the first and last rows represent the limits of realistic solutions. The first row may be thought of as the case of infinite velocity, and the last row represents infinite radius of curvature at the rear stagnation point. These results are summarized on Figure 2.

It will be noted that the infinite radius of curvature at the back of the droplet, signifying a tendency of the whole droplet to become flattened there, occurs at values of Weber number approaching one which is, in fact, the approximate experimental limit for a stable droplet. (In Ref. 1, Weber number is 4 times the definition here.) This is certainly a reasonable feature of the solution. We notice that over the range of substances considered in the calculations, the conditions of our analysis are met only for Weber numbers greater than about .3. Below that value, separated wakes would presumably be expected.

Shown also on the figure are the experimental drag coefficients from Fig. 10 of Ref. 1, which, of course, depend on the action of viscosity. The points where these experimental curves cross the calculated ones should define the droplets having minimum wakes. Figs. 2 and 4 of Ref. 1 indicate that the photographs showed minimum wake extent when the drag coefficient was a minimum. In all cases the drag minimum was at about $W' \approx 0.8$. Thus, the present calculations seem to predict a minimum value in the right range of Weber number, though the agreement is not as close as one might wish.

It is important to notice that the circulation within the droplet calculated in this paper is very small compared with the circulation that would characterize a Hill's vortex. One may perhaps conclude that any distortion of droplet shape from the spherical has a profound effect on the circulation within the droplet tending to suppress it. One may, therefore, question whether it is realistic to use a small perturbation boundary layer analysis as is done in Refs. 1 and 2 for theoretical study of viscous effects in these problems. A boundary layer study being carried out by Mr. B. Sumner at Cornell casts further doubt on this assumption, even in the case of spherical droplets.

REFERENCES

1. Winnikow, S. and Chao, B.T.: Droplet Motion in Purified Systems. Phys. Fluids, vol. 9, pp. 50-61, Jan. 1966.

2. Harper, J.F. and Moore, D.W.: The Motion of a Spherical Liquid Drop at High Reynolds Number. J. Fluid Mech., vol. 32, pp. 367-391, 1968.

3. Batchelor, G.K.: On Steady Laminar Flow with Closed Streamlines at Large Reynolds Number. Jour. Fluid Mech., vol. 1, pp. 177-190, 1956.

4. Chao, B.T.: Motion of Spherical Gas Bubbles in a Viscous Liquid at Large Reynolds Numbers. Phys. Fluids, vol. 5, pp. 69-79, 1962.

APPENDIX - SYMBOLS

A_n Coefficients of spherical harmonics (eq. 9)

a_n Dimensionless coefficients (eq. 11)

B Bond number (eq. 11)

C_D Drag coefficient

C_n Coefficients (eq. 10)

c_n Dimensionless coefficients (eq. 11)

D Drag force on drop

g Acceleration due to gravity

K Bernoulli constant (eq. 6)

k Constant related to vorticity (eq. 9)

P_n Legendre polynomials: $P_1 \equiv \mu$; $P_2 \equiv \frac{1}{2}(3\mu^2-1)$; $P_3 \equiv \frac{1}{2}(5\mu^2-3\mu)$; ...

p Pressure

$R(\theta)$ Spherical polar coordinate of surface

R_c Radius of curvature at rear stagnation point (eq. 18)

R_e Equivalent spherical drop radius (eq. 19)

U Velocity of free stream

u Radial velocity (Fig. 1)

v Velocity in θ - direction (Fig. 1)

W Weber number (eq. 11)

θ Angle measured from rear stagnation point (Fig. 1)

κ Dimensionless vorticity (eq. 11)

μ $\cos \theta$

μ_i Viscosity of fluid inside drop

μ_o Viscosity of fluid outside drop

ρ Density

σ Coefficient of surface tension

Ψ Stream function (eq. 2)

Primes: denote differentiation with respect to θ, and also redefinitions of W and B.

Subscripts:

i	Inside drop
o	Outside drop
n	Order of spherical harmonics
1	At rear stagnation point ($\theta=0$)
2	At shoulder ($\theta=\pi/2$)
3	At front stagnation point ($\theta=\pi$)

Subscript occasionally denotes partial differentiation.

TABLE

Water drops in water ($\frac{\rho_i}{\rho_o} = 1$; $\frac{\mu_i}{\mu_o} = 1$)

$\frac{R_2}{R_1}$	$\frac{R_3}{R_1}$	$\frac{R_e}{R_1}$	B'	W'	C_D	κ	a_1	a_2	a_3	c_1	c_2	c_3
1.233	1.000	1.159	0.000	0.527	0.000	-2.724	-0.375	-0.000	-0.165	-0.875	-0.000	0.062
1.284	1.300	1.246	0.040	0.340	0.621	-2.671	-0.418	0.032	-0.169	-1.022	0.094	0.040
1.406	1.600	1.392	0.064	0.376	0.907	-2.228	-0.421	0.053	-0.142	-1.400	0.328	-0.014
1.591	1.900	1.587	0.132	0.589	1.199	-1.576	-0.374	0.059	-0.099	-2.078	0.742	-0.108
1.780	2.150	1.774	0.243	0.842	1.536	-0.987	-0.286	0.051	-0.060	-2.925	1.256	-0.224

Chlorobenzene in water ($\frac{\rho_i}{\rho_o} = 1.107$; $\frac{\mu_i}{\mu_o} = 0.799$)

$\frac{R_2}{R_1}$	$\frac{R_3}{R_1}$	$\frac{R_e}{R_1}$	B'	W'	C_D	κ	a_1	a_2	a_3	c_1	c_2	c_3
1.219	1.000	1.150	0.000	0.539	0.000	-2.975	-0.403	-0.000	-0.181	-0.847	-0.000	0.058
1.289	1.350	1.260	0.039	0.350	0.592	-2.830	-0.450	0.039	-0.180	-1.046	0.125	0.028
1.426	1.650	1.418	0.068	0.438	0.825	-2.285	-0.444	0.058	-0.146	-1.474	0.387	-0.031
1.587	1.900	1.584	0.129	0.641	1.075	-1.687	-0.399	0.063	-0.106	-2.065	0.746	-0.112
1.778	2.150	1.772	0.240	0.884	1.450	-1.055	-0.305	0.054	-0.064	-2.916	1.260	-0.227

Nitrobenzene in water ($\frac{\rho_i}{\rho_o} = 1.199$; $\frac{\mu_i}{\mu_o} = 2.030$)

$\frac{R_2}{R_1}$	$\frac{R_3}{R_1}$	$\frac{R_e}{R_1}$	B'	W'	C_D	κ	a_1	a_2	a_3	c_1	c_2	c_3
1.280	1.000	1.192	0.000	0.581	0.000	-1.889	-0.274	-0.000	-0.112	-0.976	0.000	0.079
1.321	1.300	1.271	0.052	0.374	0.738	-1.918	-0.313	0.024	-0.120	-1.103	0.086	0.057
1.408	1.550	1.383	0.071	0.370	1.027	-1.704	-0.320	0.038	-0.108	-1.385	0.265	0.015
1.573	1.850	1.563	0.128	0.524	1.306	-1.262	-0.292	0.045	-0.079	-1.991	0.644	-0.074
1.750	2.100	1.741	0.225	0.757	1.582	-0.831	-0.233	0.041	-0.051	-2.768	1.127	-0.185

m-Nitrotoluene and water ($\frac{\rho_i}{\rho_o} = 1.164$; $\frac{\mu_i}{\mu_o} = 2.330$)

$\frac{R_2}{R_1}$	$\frac{R_3}{R_1}$	$\frac{R_e}{R_1}$	B'	W'	C_D	κ	a_1	a_2	a_3	c_1	c_2	c_3
1.289	1.000	1.199	0.000	0.585	0.000	-1.732	-0.254	-0.000	-0.102	-0.996	0.000	0.083
1.341	1.350	1.295	0.058	0.363	0.849	-1.747	-0.295	0.025	-0.109	-1.161	0.112	0.054
1.437	1.600	1.413	0.080	0.379	1.127	-1.522	-0.297	0.037	-0.096	-1.478	0.313	0.007
1.577	1.850	1.565	0.131	0.513	1.360	-1.174	-0.273	0.042	-0.073	-2.002	0.642	-0.070
1.751	2.100	1.742	0.226	0.744	1.623	-0.774	-0.218	0.038	-0.047	-2.776	1.124	-0.183

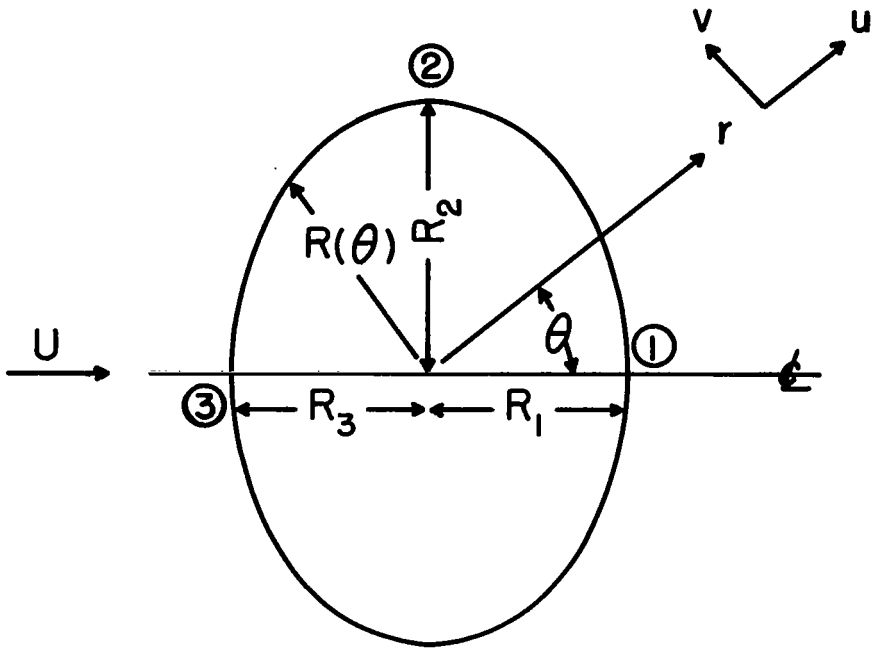

Fig. 1 Sketch of coordinates

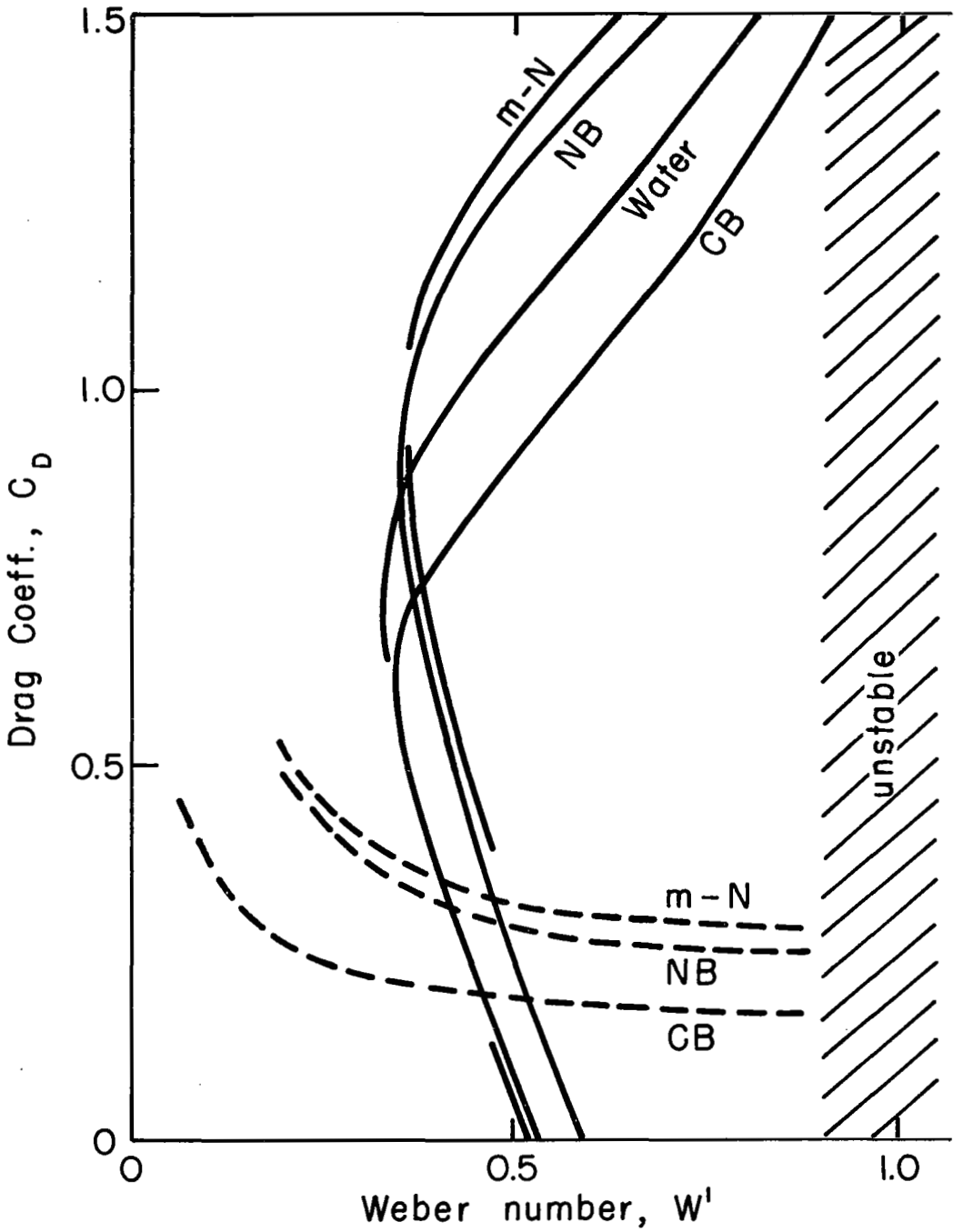

Fig. 2. Drag vs. Weber number for Water, m-Nitrotoluene (m-N), Nitrobenzene (NB), and chlorobenzene (CB) drops in water; solid lines are present calculations, dashed lines are experimental results of Ref. 1.

NASA-Langley, 1969 — 12 E-4962